Adsorbing low concentrations of Cr(VI) onto CeO_2@ZSM-5 and the adsorption kinetics, isotherms and thermodynamics

Jianrui Niu, Xiuxiu Jia, Yaqing Zhao, Yanfang Liu, Weizhang Zhong, Zengli Zhai and Zaixing Li

ABSTRACT

The CeO_2@ZSM-5 was prepared by the dipping method. We used ZSM-5 and CeO_2 as the carrier and load components, respectively. The aim was to reduce the low concentration of Cr(VI) in simulated wastewater (the concentration of Cr(VI) ranged from 0.2 to 1 mg/L). The characteristics of ZSM-5 and CeO_2@ZSM-5 samples were determined by X-ray powder diffraction (XRD), scanning electron microscopy with energy dispersive X-ray spectroscopy (SEM-EDX), X-ray photoelectron spectroscopy (XPS), Fourier transform infrared spectroscopy (FTIR) and Brunauer–Emmett–Teller (BET). Characterization results showed that the particle size, BET surface area and pore volume for CeO_2@ZSM-5 was around 0.783 nm, 421.307 m^2/g and 0.313 m^3/g, respectively. In addition, the optimum conditions were obtained by the orthogonal test, and the details were as follows: optimal pH, adsorbent dose, initial concentration of Cr(VI) and equilibrium time were 3, 5 g/L, 0.6 mg/L and 70 min respectively. The removal of Cr(VI) was 99.56% in these conditions. The pseudo-second-order model best described the adsorption kinetics of Cr(VI) onto CeO_2@ZSM-5. Isotherm data were treated according to Langmuir, Freundlich and Temkin isotherm models. The results showed that the Freundlich adsorption isotherm model fitted best in the temperature range studied. Adsorption capacity increased with temperature, showing the endothermic nature of Cr(VI) adsorption. The desorption results showed the best recovery of Cr(VI) using 0.1 M HCl.

Key words | CeO_2@zsm-5, Cr(VI) adsorption, kinetics, isotherms, thermodynamics

Jianrui Niu
Xiuxiu Jia
Yaqing Zhao
Yanfang Liu
Weizhang Zhong
Zengli Zhai
Zaixing Li (corresponding author)
College of Environmental Science and Engineering,
Hebei University of Science and Technology,
Shijiazhuang 050018,
China
E-mail: *lizaixing@hebust.edu.cn*

INTRODUCTION

Chromium is found in the sewage discharge of some enterprises, such as the production of leather, electroplating, printing, dyeing and the chemical industry. Chromium oxide is usually used as a paint and colorant. It can also produce chromium wastewater. Cr(III) and Cr(VI) are two common oxidation states of chromium found in the environment (Sharma *et al.* 2017), but Cr(VI) cannot be naturally degraded. It is highly carcinogenic and oxidative, and its toxicity is 100 times that of Cr(III). To sum up, if Cr(VI) cannot be processed in a timely and effective manner, it will cause serious harm to the human body and the environment.

There are many ways to remove Cr(VI), such as the adsorption method, chemical method, biological method, ion exchange method, electrolytic method, membrane separation method. The adsorption method is a relatively mature approach and is emerging as a potentially preferred alternative for the removal of heavy metals. Compared with other methods (Alothman *et al.* 2013), adsorption is the most efficient because of ease of operation, high-quality treated effluent and the fact that the adsorbent can be regenerated. There is much research on various chromium adsorption materials, the most commonly used being activated carbon (Alothman *et al.* 2013), graphite (Gopalakrishnan *et al.* 2015), carbon nanotubes (Mubarak *et al.* 2016) and zeolite (Choi *et al.* 2016), etc.

However, because of the presence of water and impurities in the channels, the adsorption capacity of natural adsorption materials is low (Hall *et al.* 1966). Choi *et al.* modified zeolite by replacing Si(IV) and Al(III) sites in the lattice with exchangeable cations such as sodium, magnesium, potassium, or calcium, resulting in a net negative charge (Choi *et al.* 2016). The Mg-modified adsorbent had a cadmium removal of more than 98% at an optimum pH

doi: 10.2166/wst.2018.157

of 7. In addition, the adsorption capacity of Mg-zeolite was found to be 1.5–2.0 times higher than that of natural zeolite. Therefore, modified materials are mostly employed in practical applications. Since CeO_2 (ceria) has high oxidation and thermal stability, it tends to modify various catalysts to improve the activity of the catalyst (Salerno *et al.* 2017). The surface area and the number of bulk/sub-surface defects in the ceria seem to be the main properties determining the catalytic activity. Rivas *et al.* found that the introduction of CeO_2 on the zeolite HZSM-5 produced high catalytic activity and stability (Rivas *et al.* 2013). The zeolite ZSM-5 is a traditional molecular sieve developed by Mobil in the 1970s. Its high surface area and the fact that it is hydrophilic make it suitable for the sequestration of chromium. However, there have been few reports of applying CeO_2 to modifying a molecular sieve to remove heavy metal pollution in aqueous solutions. Therefore, this paper makes an attempt on it.

The present paper reports the results for the kinetic, equilibrium and thermodynamics studies of Cr(VI) adsorption onto CeO_2@ZSM-5. Since the effectiveness of adsorption relies strongly on operational conditions, parameters that may affect the adsorption including adsorbent dose, initial concentration, contact time and pH were evaluated. Both kinetic and equilibrium isotherm models were used to establish the process of adsorption. The results of this study showed that CeO_2@ZSM-5 was easy to prepare and efficient for treating low concentrations of chromium.

MATERIALS AND METHODS

Raw material and reagents

ZSM-5 (Si/Al = 38) was purchased from Nankai University Catalyst Co., Ltd and was not processed before use. Cerium nitrate ($Ce(NO_3)_3{\cdot}6H_2O$), sodium hydroxide (NaOH), anhydrous ethanol (CH_3CH_2OH) and potassium dichromate ($K_2Cr_2O_7$) were purchased from Tianjin Yongda Chemical Reagent Co., Ltd. LH-Cr1 and LH-Cr2 were used as a standard reagents for determining chromium concentration and bought from Beijing Llianhua Environmental Protection Technology Co., Ltd. All the reagents were analytical grade, except for ZSM-5, which was chemically pure.

Preparation of CeO_2@ZSM-5

CeO_2@ZSM-5 were prepared by impregnation of the ZSM-5 (3 g) with an aqueous solution (200 mL) of cerium nitrate for 12 hours at room temperature. Simple ZSM-5 modified by CeO_2 loading (11 wt%) was obtained. A rotating evaporator was used to remove the moisture. The sample was then dried at 110 °C for 2 hours followed by calcination at 550 °C for 3 hours. The resulting CeO_2@ZSM-5 was characterised using several analytical techniques.

Characterization techniques

X-ray powder diffraction (XRD) patterns were recorded with a D/MAX-2500 diffractometer using CuKα (0.154 nm) radiation in the region between 5 and 55° (2θ) at a speed of 2° per min. Brunauer–Emmett–Teller (BET) surface area, pore volume, micropore surface area and average pore diameter were determined by nitrogen adsorption at 77 K, using 3Flex analyzer (Micromeritics, ASIQM000100-6), surface area and pore size analyzer. The surfaces of the natural zeolite and CeO_2@ZSM-5 were imaged using a scanning electron microscope (SEM), JEOL 6300F. Elemental analysis was done by an energy dispersive X-ray (EDX) spectroscopy instrument equipped with SEM. The Fourier transform infrared spectroscopy (FTIR) spectra of the adsorbent were recorded with the KBr pellet method using a Nicolet 6700 FTIR spectrometer. X-ray photoelectron spectroscopy (XPS) analysis was performed using an X-ray photoelectron spectrometer (EscaLab 250xi).

Adsorption analysis

A stock solution of Cr(VI) (100 mg/L) was prepared using potassium dichromate dissolved in double-distilled water. All working solutions of varying concentrations were obtained by successive dilution. The pH of the solution was adjusted to the required value using 0.1 M HCl and 0.1 M NaOH.

Adsorption experiments for ZSM-5 and CeO_2@ZSM-5 were undertaken by the batch equilibrium technique. A solution with a known initial concentration of Cr(VI) was prepared and a certain mass of the ZSM-5 or CeO_2@ZSM-5 and 100 mL of the Cr(VI) solution was added to the batch adsorber. Influencing factors: adsorption doses, initial concentrations of Cr(VI), pH and contact time were varied from 0.1 to 0.9 g, 0.1 to 1 mg/L, 2 to 11 and 20 to 100 min, respectively. The reaction was placed in a constant temperature oscillator which was set at a temperature of 25 °C and a speed of 150 rpm for 60 min. The concentration of Cr(VI) was established after suction filtration. We also did the orthogonal experiment to optimize the conditions. The residual chromium concentration was determined by heavy metal multi-parameter tester.

The adsorption capacities were calculated based on the differences in the concentrations of solutes before and after the experiment according to Equations (1) and (2):

$$q_e = \frac{(C_0 - C_e) \cdot v}{m} \quad (1)$$

$$E = \frac{(C_0 - C_e)}{C_0} \times 100\% \quad (2)$$

where q_e is the concentration of the adsorbed solute (mg/g); E is the removal rate (%); C_0 and C_e are the initial and final (equilibrium) concentrations of Cr(VI) (mg/L); v (ml) is the volume of the solution and m (g) is the mass of adsorbent.

RESULT AND DISCUSSION

Structure and morphology analysis

As shown in Table 1, the surface area and pore volume of ZSM-5 decreased when it was modified with CeO_2. This was caused by the active sites obstructing some of the main channels of ZSM-5, which impeded the diffusion of N_2 through these channels. The average pore diameter of ZSM-5 increased when it was modified with CeO_2. A probable explanation is that the CeO_2 blocked a large proportion the smallest pore diameters, therefore the average pore diameter increased. Another explanation is that the high temperature of calcination caused some of the small holes to collapse (Wu *et al.* 2015). After absorbing Cr(VI), the surface area and pore volume of CeO_2@ZSM-5 all have a little decrease compared to before. The nitrogen sorption isotherms of the ZSM-5 (Figure 1(a)) and CeO_2@ZSM-5 (Figure 1(b)) show a lag ring is formed when P/P_0 is between 0.4 and 0.9.

Table 1 | Textural parameters of the ZSM-5 and CeO_2@ZSM-5 employed in this study

Adsorbent	A_{BET} m^2/g	Pore volume m^3/g	D spacing nm
ZSM-5	421.307	0.371	0.744
ZSM-5(Cr(VI))	416.245	0.302	0.647
CeO_2@ZSM-5	558.532	0.313	0.783
CeO_2@ZSM-5(Cr(VI))	550.458	0.279	0.745

Figure 2(a) shows that the relative intensity of the quartz peak, 2θ around 28.55, 33.07 and 47.48, increased when ZSM-5 was modified with CeO_2. These three 2θ angles can be indexed to the crystal plane diffraction peaks to (111), (200) and (220), respectively. Those typical peaks of CeO_2 indicated that Ce had been successfully loaded onto ZSM-5. The same set of characteristic peaks was also observed for CeO_2@ZSM-5, indicating that ZSM-5 maintained its original structure. This conclusion matches well with some previous studies (Liu *et al.* 2017).

Figure 2(b) shows the FTIR spectra of CeO_2@ZSM-5 before and after the Cr(VI) adsorption. The peaks at 796 cm^{-1}, 1,099 cm^{-1} and 3,448 cm^{-1} were assigned to the Al-O stretching, Si-O stretching and -OH stretching vibrations. The peak observed at about 452 cm^{-1} was ascribed to the occurrence of Ce-O stretching (Liu *et al.* 2017; Sharma *et al.* 2017).The occurrence of the above-mentioned peaks revealed the cross-linking of Ce and ZSM-5. But after the adsorption of Cr(VI), the intensities

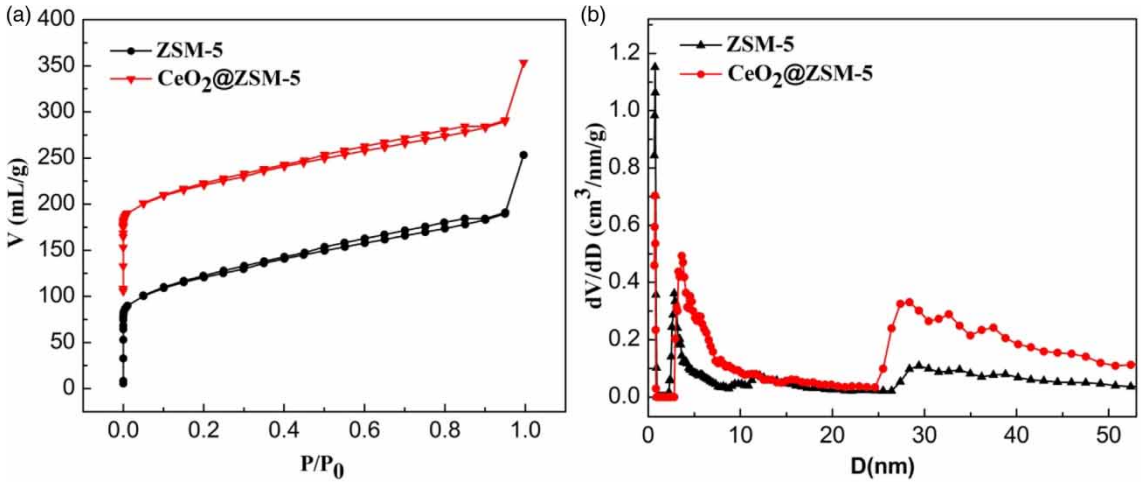

Figure 1 | (a) Adsorption/desorption isotherms of nitrogen at 77 K for ZSM-5 and CeO_2@ZSM-5; (b) BET pore-size distribution.

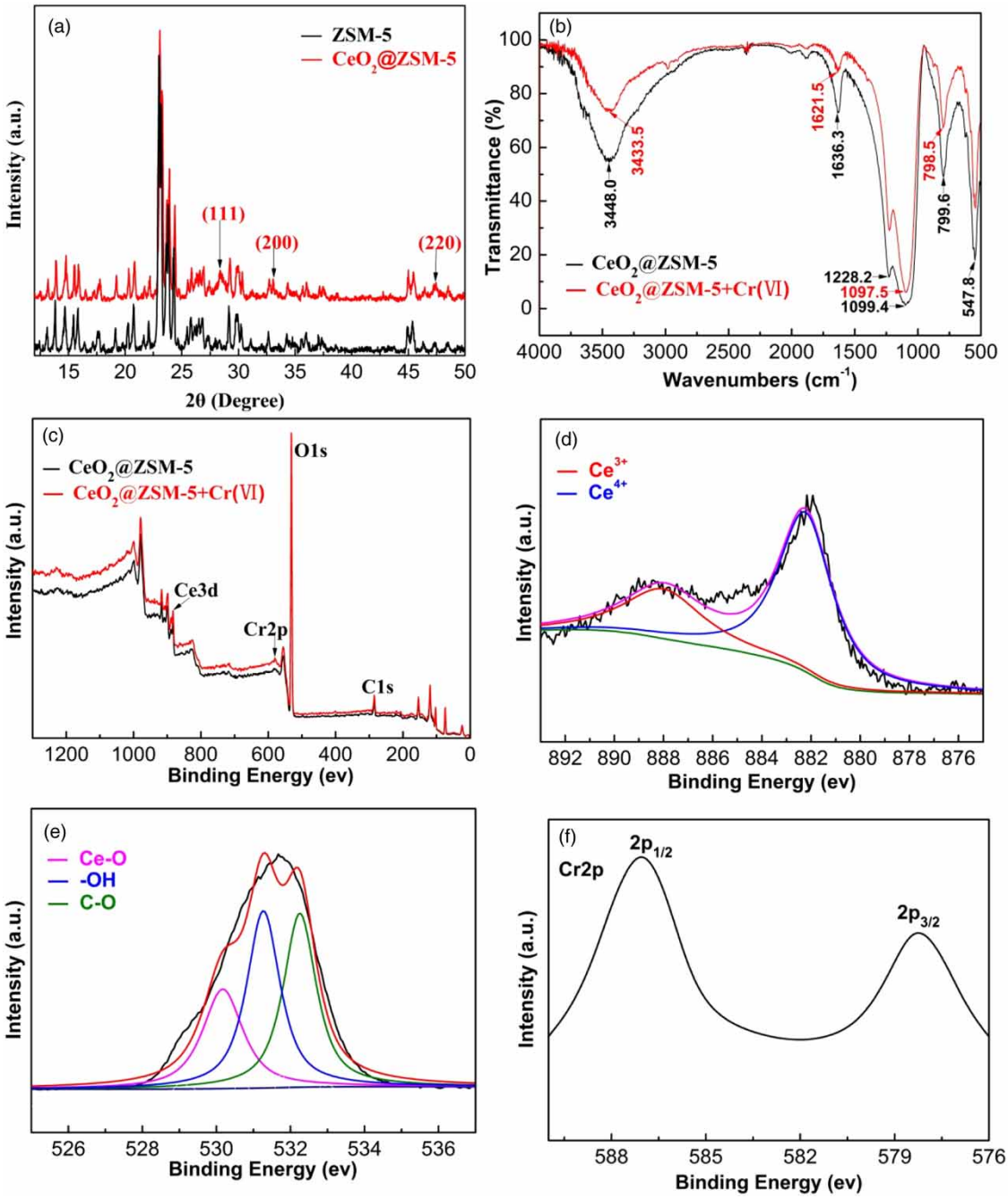

Figure 2 | (a) XRD pattern; (b) FTIR spectra; (c) XPS full spectrum; (d) high-resolution XPS spectrum for (d) Ce; (e) O; (f) Cr.

and position of some peaks (Ce-O, Al-O, and Si-O) changed, which indicated that those groups were responsible for the adsorption of Cr(VI) onto CeO_2@ZSM-5.

The surface elemental composition of CeO_2@ZSM-5 was determined using XPS analysis, as shown in Figure 2(c), which revealed the presence of Ce and O elements in the CeO_2@ZSM-5. The high-resolution spectrum of Ce3d is shown in Figure 2(d); two types of Ce atoms are present: Ce^{3+} (888.02 eV) and Ce^{4+} (882.25 eV). As shown in Figure 2(e), the O1 s spectrum of CeO_2@ZSM-5 could be fitted and de-convoluted into three different peaks, corresponding to C-O (532.75), -OH (531.18 eV) and Ce-O (530.02 eV) (Naushad *et al.* 2017). The adsorption of Cr(VI) onto CeO_2@ZSM-5 was also supported using XPS.

As shown in Figure 2(f), the appearance of the $Cr2p_{1/2}$ and $Cr2p_{3/2}$ spectrum after the adsorption demonstrated that Cr(VI) was adsorbed onto CeO_2@ZSM-5.

To further study the material, SEM-EDX elemental mapping was performed to show the difference between Cr(VI) distribution inside and outside the pores. The SEM images revealed information about the details of the surface and morphology of the particles. Figure 3(a) displays partially developed crystalline laminar habits and conglomerates of compact crystals. There were many tiny pores between particles. Some of them showed a reunion phenomenon, which suggested a large surface polarity and specific surface area of ZSM-5 (Al-Othman *et al.* 2012). Figure 3(c) shows that there was no obvious change in crystalline structure, maintaining the basic skeleton structure and larger specific surface area of CeO_2@ZSM-5, which indicated that there was no obvious damage to the basic skeleton of ZSM-5 after the modification. The comparison of Figure 3(b) and 3(d) shows that some fine particles adhered to the surface of ZSM-5 after the modification, indicating that CeO_2 had been successfully loaded onto the surface of ZSM-5, which matched well with the BET and XRD results.

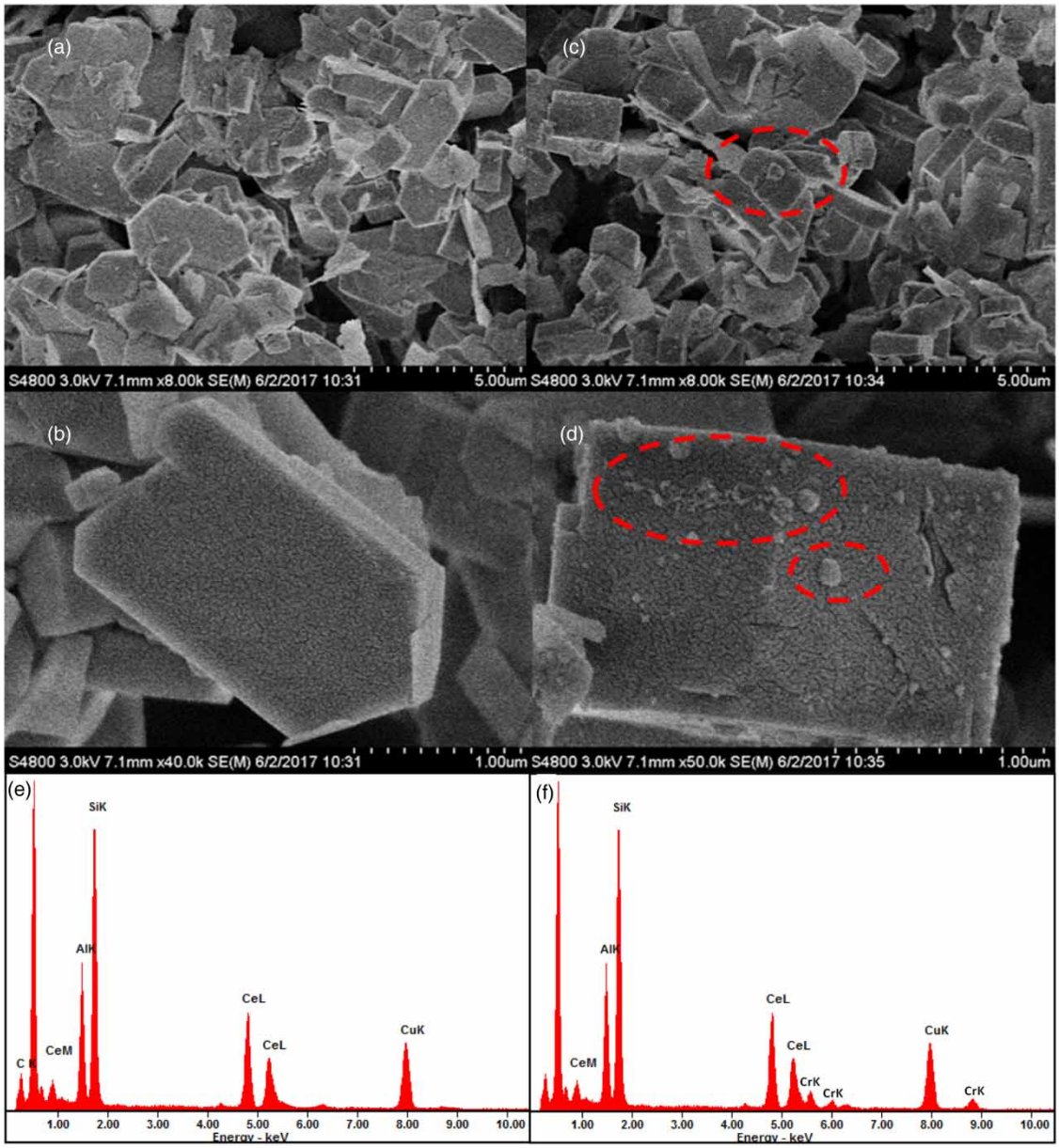

Figure 3 | (a), (b) SEM photographs of ZSM-5; (c), (d) SEM photographs of CeO_2@ZSM-5; (e) EDX spectrum of CeO_2@ZSM-5 and (f) spectrum of CeO_2@ZSM-5 with Cr(VI) adsorption.

Figure 3(e) and 3(f) show the EDX spectra of the two samples (CeO_2@ZSM-5 before and after the absorption of Cr(VI)). Because the pore area occupied a small percentage in the images, elemental mapping would not work. Here, only EDX spectrum was used to identify if there was any Cr(VI) on the surfaces inside the pores (Dai *et al.* 2016). Comparing Figure 3(e) with 3(f), it can be seen that there were some peaks inside the pores of CeO_2-@ZSM-5 attributed to Cr(VI) in the EDX spectrum. This suggested that Cr(VI) had been successfully adsorbed onto CeO_2@ZSM-5.

Effect of pH and adsorption mechanism

The solution pH is one of the most important parameters affecting the adsorption process (Alothman *et al.* 2013). The pH determines the surface charge of the adsorbent, the degree of ionization and adsorbent characteristics. In order to evaluate the effect of pH on the uptake of hexavalent chromium, 0.5 g of adsorbent was mixed with 100 mL of the chromium solution with initial concentration of 0.6 mg/L and different pH values (from 3 to 11) and shaken at room temperature for 60 min.

As shown in Figure 4(a), the percentage removal of Cr(VI) was 99% and 89% after adsorption onto CeO_2@ZSM-5 and ZSM-5, respectively, indicating that the adsorption capacity of CeO_2@ZSM-5 was greater than ZSM-5. Within the range of pH values from 3 to 11, the adsorption capacity decreased drastically with increasing pH. This suggests that the adsorption of the adsorbent is clearly pH dependent. The CeO_2@ZSM-5 sample could remove 99% of Cr(VI) in acidic conditions (pH = 3) while only 40% in alkaline conditions (pH = 11). Hence, the removal of Cr(VI) was relatively higher in the lower pH ranges. The adsorption processes are hindered at high pH because of the competitive adsorption between OH^- and $Cr_2O_4^{2-}$ (Kumar *et al.* 2016). Analogous results have been achieved by other authors (Awual *et al.* 2016; Kenawy *et al.* 2017).

As per Figure 5(a), there was large number of H^+ ions at lower pH, which neutralized the negatively charged adsorbent surface and thereby increased the diffusion of chromate ions into the bulk of the adsorbent (Rao *et al.* 2002). It has been reported by other researchers that at pH 3–4, the dominant form of Cr(VI) is $HCrO_4^-$ (Alothman *et al.* 2013). So, Cr(VI) was adsorbed on the surface of

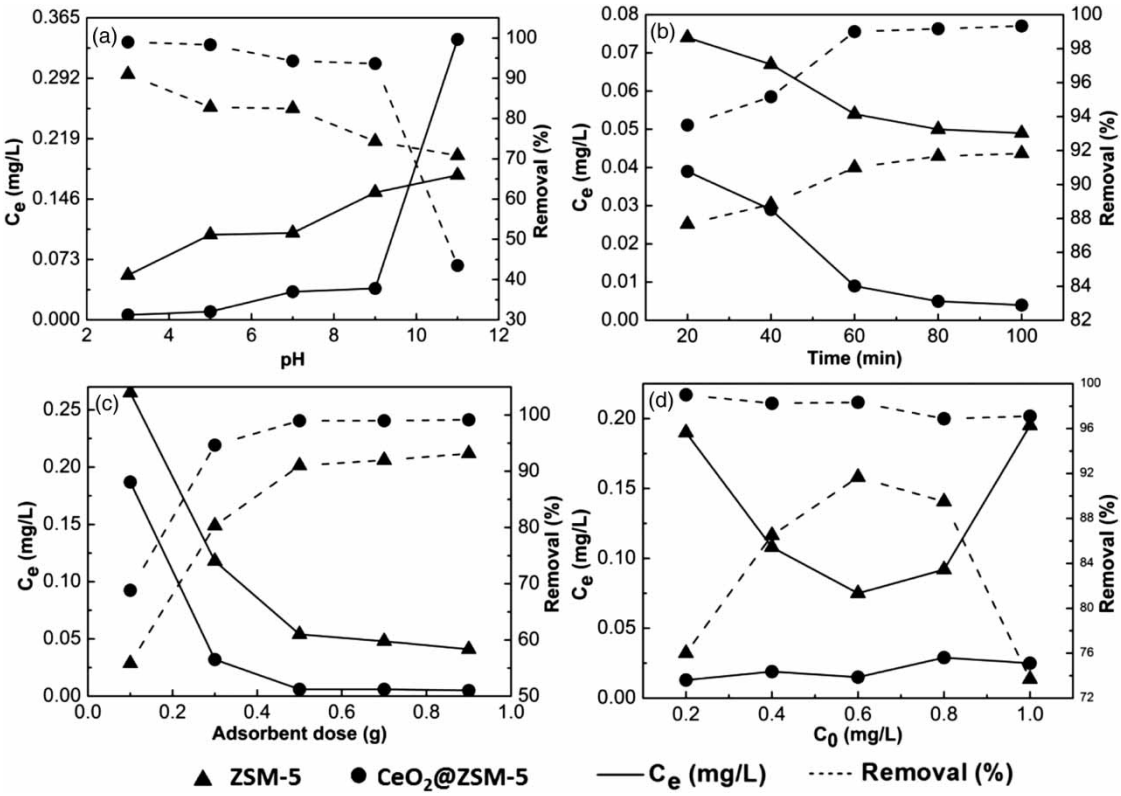

Figure 4 | Effect of (a) initial solution pH; (b) contact time; (c) adsorbent dose; (d) initial concentration on the removal of Cr(VI) onto ZSM-5 and CeO_2@ZSM-5.

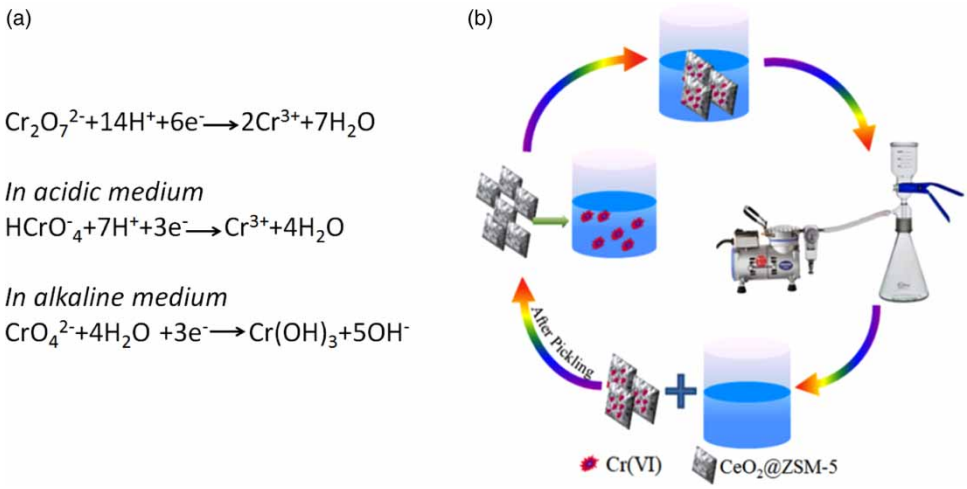

Figure 5 | (a) Mechanism for the adsorption of Cr(VI) onto CeO_2@ZSM-5; (b) entire cycle.

CeO_2@ZSM-5 mostly in the form of $HCrO_4^-$. Beyond that, it can be inferred that surface adsorption is not the only mechanism involved in the adsorption process. At lower pH, protons (H^+) adsorbed on the surfaces of CeO_2@ZSM-5 bring about more positive charges and thereby enhance the electrostatic attraction between the surfaces and negatively charged Cr(VI) anions. Also, higher acid concentrations restrain hydrolysis of the chromium ions (Zhou *et al.* 2010). The entire cycle process of this study is shown in Figure 5(b).

Effect of contact time and adsorption kinetics

In order to evaluate the effect of contact time, 0.5 g of adsorbent was mixed with 100 ml of the chromium solution with an initial concentration of 0.6 mg/L at pH 3 and shaken at room temperature for 20–100 min. Figure 4(b) shows the effect of contact time on the uptake of chromium. As can be seen in this figure, the uptake of chromium ions increases with increasing contact time and reaches equilibrium after 70 min. Actually, the adsorption rate was expected to be very rapid initially and then slowly decrease until it reached equilibrium in 70 min, caused by adsorbent saturation. With increasing contact time, the uptake of chromium remained almost constant and the removal rate was 99.24%, which is close to 100%.

To investigate the mechanism of adsorption processes, kinetic models were used to analyse the experimental data. Several kinetic models such as pseudo-first-order and pseudo-second-order have been applied to find the adsorption mechanism. The equation of the two kinetic models is expressed as follows:

The pseudo-first-order equation is given as Equation (3):

$$\lg(Q_e - Q_t) = \lg Q_e - \frac{k_1}{2.303} \cdot t \quad (3)$$

The pseudo-second-order equation is given as Equation (4):

$$\frac{t}{Q_t} = \frac{1}{k_2 Q_e^2} + \frac{1}{Q_e} \cdot t \quad (4)$$

where Q_e and Q_t are the amounts of adsorbed Cr(VI) on the adsorbent at equilibrium and at time t, respectively (mg/g), and k_1 is the first-order adsorption rate constant (min^{-1}), k_2 is the second-order adsorption rate constant (g/(mg·min)), and Q_e is the adsorption capacity calculated by the pseudo-second-order kinetic model (mg/g).

The regression correlation coefficients and constants of the pseudo-first-order and pseudo-second-order kinetic models are shown in Table 2. As can be seen in this table,

Table 2 | Adsorption kinetics for the adsorption of Cr(VI) onto CeO_2@ZSM-5

	Pseudo-first-order			Pseudo-second-order		
C0 (mg/L)	k_1 (min^{-1})	R^2	q_e (mg/g)	k_2 (g/mg·min)	R^2	q_e (mg/g)
0.5	0.0252	0.9770	0.0156	0.0939	0.9917	0.1755
0.6	0.0308	0.9572	0.2099	0.0293	0.9991	0.2976
0.7	0.0271	0.9739	0.3958	0.0160	0.9903	0.4135

the theoretical adsorption of hexavalent chromium obtained by the pseudo-second-order kinetic model were 0.1755 mg/g, 0.2976 mg/g, 0.4135 mg/g at the initial concentration of 0.5 mg/L, 0.6 mg/L and 0.7 mg/L, respectively, which was very close to the actual measurement of hexavalent chromium equilibrium adsorption 0.1738 mg/g, 0.2885 mg/g, 0.4069 mg/g. However, they are very different from those of the pseudo-first-order kinetic model. In addition to this, the fitting degree of the pseudo-second-order kinetic model was 0.99 in the three concentrations, so the kinetic adsorption can be very well described by the pseudo-second-order equation, which indicates that the adsorption rate of CeO_2@ZSM-5 for Cr(VI) is directly proportional to the square of the unoccupied adsorption site of the adsorbent. Other researchers (Naushad *et al.* 2016, 2017) have also been reported similar results for the adsorption of Cr(VI) (Figure 6).

Effect of adsorbent dose

The effect of adsorbent dose on the uptake of chromium is shown in Figure 4(c). The experiments were done using different amounts of adsorbent (0.1–0.9 g) at the optimum pH and contact time. With the increase in adsorbent from 0.1 to 0.5 g, the uptake of Cr(VI) increases because the number of available adsorption sites increases. This phenomenon is consistent with the kinetic studies, which indicate that the adsorption rate is directly proportional to the square of the unoccupied adsorption sites of the adsorbent. However, for higher doses (>0.5 g), the uptake efficiency is almost constant because all of the adsorbate had already sorbed to the active sites of adsorbent. The removal rate of ZSM-5 and CeO_2@ZSM-5 is 93% and 99% respectively when the adsorbent dose is 9 g/L, while it is 91% and 99% when the amount is 5 g/L. It can be seen that the removal rates are almost indistinguishable in both cases. Maximum uptake of chromium occurred when using 0.5 g adsorbent. Therefore it was chosen as the adsorbent optimum amount for further experiments. This result was expected because for a fixed initial solute concentration, increasing amount of adsorbent provides greater surface area (or adsorption sites) (Alothman *et al.* 2013).

Effect of the initial concentration of Cr(VI)

The uptake of Cr(VI) by ZSM-5 and CeO_2@ZSM-5 was studied in the range of 0.2–1 mg/L, while the other conditions such as adsorbent dose, pH, and contact time were constant. The results are presented in Figure 4(d). The removal efficiency is decreased with the increasing concentration of Cr(VI) in solution. The active sites of the adsorbent were saturated over time. CeO_2@ZSM-5 showed an excellent removal efficiency in the treatment of low concentration wastewater, and the removal rate was 97.52%. In the initial concentration of 0.6 mg/L, the removal rate of Cr(VI) reached 91.67% when using ZSM-5 as the adsorbent. As the concentration went up, the removal rate decreased, so 0.6 mg/L was chosen as the optimal initial concentration.

Conditions optimization

In view of the effect of various factors on the percentage removal, four major factors were mentioned as follows (Table 3): initial concentration of Cr(VI) (A), pH value (B), CeO_2@ZSM-5 dosage (C) and reaction time (min) (D). In this experiment, an $L_9(3)^4$ orthogonal experiment was designed, and the optimal treatment conditions were obtained by using the removal rate of Cr(VI) as the objective.

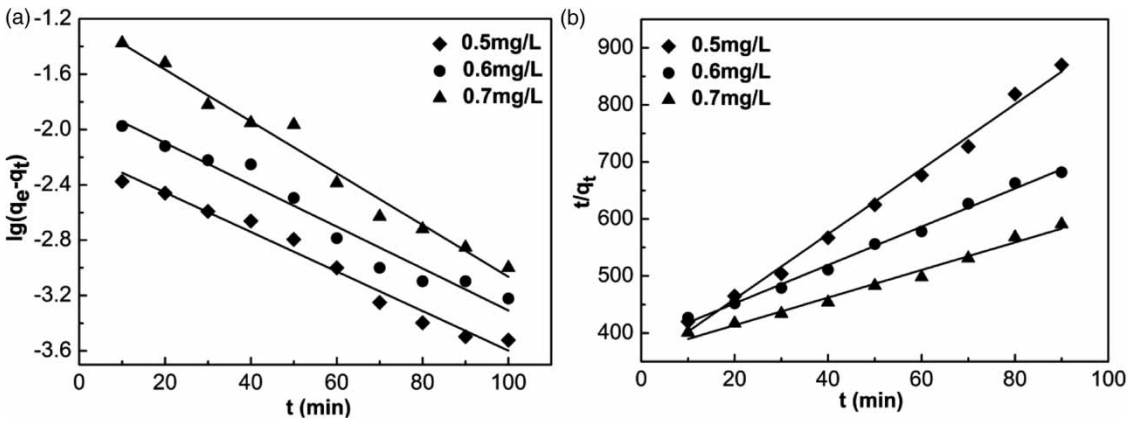

Figure 6 | (a) Pseudo-first-order, (b) pseudo-second-order sorption kinetics of Cr(VI) onto CeO_2@ZSM-5.

Table 3 | The factors of orthogonal experiment

Factors	A Initial concentration (mg/L)	B pH	C Adsorbent dose (g/L)	D Contact time (min)
1	0.4	2	3	50
2	0.5	3	4	60
3	0.6	4	5	70

As can be seen from Table 4, the four influencing factors were ranked according to their influence: pH > initial concentration > reaction time > adsorbent dose. The pH value was the main factor affecting the adsorption and the optimum technological conditions for the reaction were $A_3B_2C_2D_3$ through the above experiments. To be specific, the initial concentration, pH, adsorbent dose and reaction time were 0.6 mg/L, 3, 0.5 g/L, and 70 min, respectively, and the removal rate of hexavalent chromium was 99.56% under these conditions.

Adsorption isotherms

Adsorption isotherm studies are important for identifying the efficacy of adsorption. Some well-known ones are Freundlich, Langmuir, Temkin and Redlich–Peterson (Sharma *et al.* 2017). In this study, Langmuir, Freundlich and Temkin isotherm models were used to establish the adsorption equilibrium between the adsorbent and metal ions. For this purpose, 100 ml of the chromium solution with concentrations of 0.1, 0.2, 0.3, 0.4, 0.5, 0.6, 0.7, 0.8, 0.9 and 1 mg/L were prepared at room temperature and the adsorption of hexavalent chromium was calculated by Equation (5) at pH 3, using 0.5 g adsorbent and a contact time of 70 min.

Table 4 | The results and analysis of orthogonal experiments

	Influencing factor				
Serial number	A	B	C	D	Removal rate(%)
1	1	1	1	1	91.75
2	1	2	2	2	99.50
3	1	3	3	3	98.75
4	2	1	2	3	95.40
5	2	2	3	1	98.60
6	2	3	1	2	98.60
7	3	1	3	2	83.00
8	3	2	1	3	95.00
9	3	3	2	1	94.00
K_1	92.261	90.050	94.450	94.783	
K_2	95.867	97.700	96.300	93.033	
K_3	96.657	96.450	93.450	96.383	
R^2	6.200	7.650	2.850	3.350	

The Langmuir model assumes that a monomolecular layer is formed when adsorption takes place without any interaction between the adsorbed molecules. The Langmuir model can be represented as:

$$q_e = \frac{q_m K_L C_e}{1 + K_L C_e} \tag{5}$$

The linearized form of the Langmuir equation is Equation (6):

$$\frac{1}{Q_e} = \frac{1}{Q_m} + \frac{1}{K_L Q_m} \cdot \frac{1}{C_e} \tag{6}$$

The essential features of a Langmuir isotherm can be expressed in terms of a dimensionless constant separation factor or equilibrium parameter, R_L, which is defined by Hall *et al.* (1966) as Equation (7):

$$R_L = \frac{1}{1 + K_L C_0} \tag{7}$$

where C_e is the equilibrium concentration (mg/L), q_e the amount of metal ion sorbed (mg/g), q_m is q_e for a complete monolayer (mg/g), K_L is a constant related to the affinity of the binding sites (L/mg). When $0 < R_L < 1$, the adsorption is in a favorable direction, while it is negative when $R_L > 1$.

The experimental data were plotted as C_e/q_e versus C_e and shown in Figure 7(a). Values of the Langmuir constants q_m and K_L were obtained by linear regression and shown in Table 5.

The Freundlich isotherm is an empirical equation assuming that the adsorption process takes place on heterogeneous surfaces and adsorption capacity is related to the concentration of Cr(VI) at equilibrium.

This equation can be written in the linear form given as below (8) and (9):

$$q_e = K_F C_e^{1/n} \tag{8}$$

$$\lg Q_e = \lg k + \frac{1}{n} \lg C_e \tag{9}$$

where q_e, and C_e are the equilibrium concentrations of Cr(VI) in the adsorbed (mg/g) and liquid phases (mg/L),

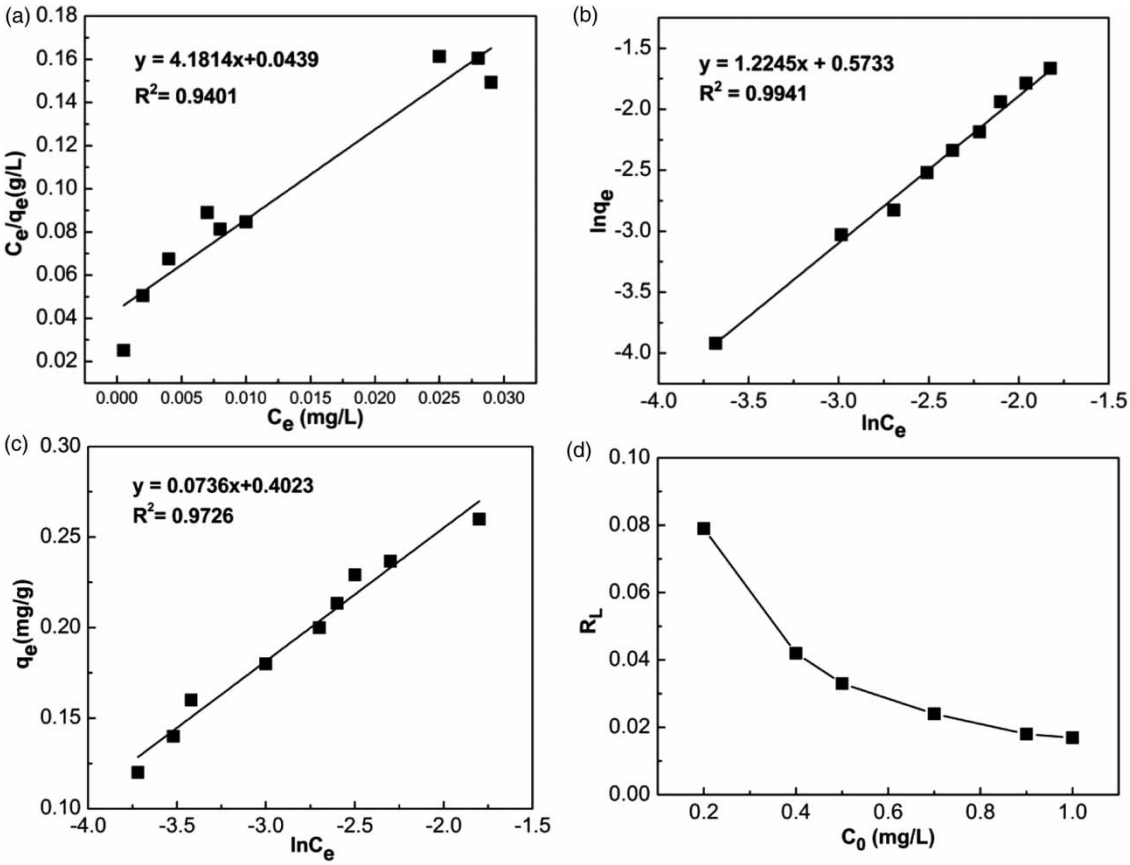

Figure 7 | (a) Langmuir, (b) Freundlich, (c) Temkin isotherm models for the adsorption of Cr(VI) onto CeO_2@ZSM-5 and (d) R_L of different initial concentrations.

respectively, K_F and n are the Freundlich constants which are related to adsorption capacity and intensity, respectively. The experimental data were plotted as lnq_e versus lnC_e and shown in Figure 7(b). To determine the maximum sorption capacity, it is necessary to operate with constant initial concentration C_0 and variable weight of sorbent, thus lgq_e is the extrapolated value of lgq for $C = C_0$ (Djeribi & Hamdaoui 2008).

The Temkin isotherm model assumes that the adsorption energy decreases linearly with the surface coverage due to adsorbent–adsorbate interactions. The linear form of the Temkin isotherm model is described as follows:

$$q_e = B_t \ln(K_T) + B_t \ln(C_e) \quad (10)$$

where B_t (heat of sorption) is RT/b and K_T is the equilibrium binding constant (L/mg). The Temkin parameters B_t and K_T were determined from the plot of q_e versus lnC_e.

Linear plots for the Temkin adsorption isotherm are shown in Figure 7(c) for Cr(VI) adsorption on CeO_2@ZSM-5. The Temkin constants were determined from the slope and intercept of a linear plot of q_e versus lnC_e and are given in Table 5.

As shown in Table 5, the fitting parameters of the Langmuir model, Freundlich model and Temkin model were 0.9401, 0.9941 and 0.9726, respectively. This implies that the Freundlich model had a higher correlation coefficient value as compared to the Langmuir and Temkin isotherms. Other researchers (Naushad *et al.* 2016) have also reported

Table 5 | Isotherm parameters for the adsorption of Cr(VI) metal ion onto CeO_2@ZSM-5

Langmuir model			Freundlich model			Temkin model		
q_m(mg/g)	K_L(L/mg)	R^2	n	K_F(mg/g)	R^2	B_t	K_T(L/mg)	R^2
0.2392	58.1489	0.9401	1.2046	1.6785	0.9941	0.0736	236.5	0.9726

similar results for the adsorption of Cr(VI). Figure 7(d) shows that the $R_L<1$, which indicate that the adsorption process is in a favorable direction. The parameter n in the Freundlich model is 1.2046 (>1), indicating that the adsorption process is spontaneous, which is consistent with the conclusion that the adsorption is in the favorable direction when $R_L<1$.

Effect of temperature and thermodynamics

Temperature has a distinct effect on the adsorption capacity of an adsorbent. The adsorption of Cr(VI) onto CeO_2@ZSM-5 was analyzed at different temperatures (288, 298, 308 and 318 K). The thermodynamic parameters, such as ΔH° (enthalpy change), ΔG° (standard free energy), and ΔS° (entropy change) were calculated. The values of ΔH° and ΔS° were obtained from the slopes and intercepts of the plots of *lnKc* versus *1/T* (as shown in Figure 8) by the following equation:

$$lnK_c = -\frac{\Delta H^\circ}{RT} + \frac{\Delta S^\circ}{R} \quad (11)$$

The values of ΔG° was calculated using the following equation:

$$\Delta G^\circ = \Delta H^\circ - T\Delta S^\circ \quad (12)$$

where R (8.314 kJ/molK) is the gas constant, T (degrees Kelvin), absolute temperature, and Kc (L/mg), the standard thermodynamic equilibrium constant defined by C_0-C_e/C_e. It may be observed from Table 6 that the value of ΔG° was negative, indicating the spontaneous nature of the adsorption process. The values of ΔG° were more negative at higher temperatures, showing that higher temperature favored the adsorption of Cr(VI) onto CeO_2@ZSM-5. The positive value of ΔS° revealed an increase in the randomness at the solid/solution interface during the adsorption process. Value of ΔH° was positive, indicating the endothermic nature of the adsorption. Other researchers (Al-Othman *et al.* 2012; Alqadami *et al.* 2017) have also reported similar results for the adsorption of Cr(VI).

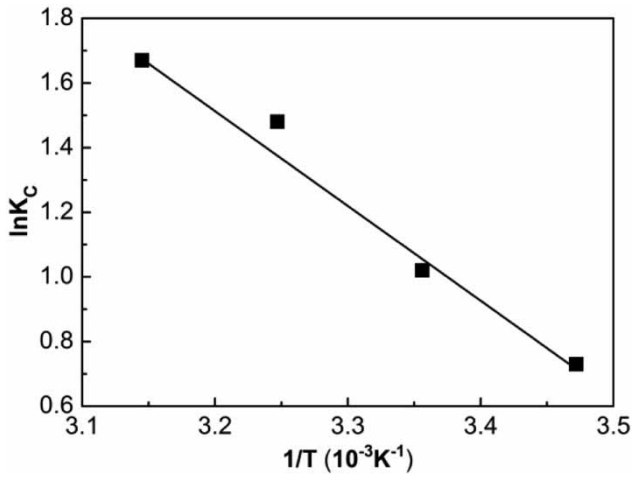

Figure 8 | Plot of *lnKc* versus *1/T* for Cr(VI) adsorption on CeO_2@ZSM-5.

Table 6 | Thermodynamic parameters for Cr(VI) adsorption on CeO_2@ZSM-5

T (K)	$-\Delta G^\circ$ (kJ/mol)	ΔH° (kJ/mol)	ΔS° [J/(mol K)]
288	1.03	30.29	109.34
298	1.52		
308	2.18		
318	2.74		

Effect of coexisting ions

Industrial discharges may contain a large number of other ions that may have a competitive effect on Cr(VI) adsorption, such as Mg^{2+}, Ca^{2+}, Na^{+}, K^{+}, Cu^{2+} and Fe^{3+}. Thus the adsorption of Cr(VI) onto CeO_2@ZSM-5 was studied in the presence of these ions. The experiment was carried out in a batch mode where 0.5 g of the adsorbent was in 100 mL of aqueous solution containing Cr(VI) ions and known quantities of those coexisting ions. The adsorption of Cr(VI) onto CeO_2@ZSM-5 was 99.56% before addition of any ions. On addition of those ions, the adsorption of Cr(VI) onto CeO_2@ZSM-5 was slightly decreased in the order Na^{+} (97.15%) > K^{+}(95.21%) > Mg^{2+}(93.31%) > Ca^{2+}(90.43%) > Fe^{3+}(86.68%) > Cu^{2+}(86.49%) (Figure 9(a)). Thus, CeO_2@ZSM-5 could be very well used for Cr(VI) removal in the presence of these competing ions. This result was in accordance with the hydrated ion radius. The ions with smaller hydrated radius easily enter the pores of the adsorbent, resulted in higher adsorption (Sharma *et al.* 2017).

Desorption studies

To assess the material feasibility for potential application, it must be assessed not only on adsorptive ability, but also on regeneration and reusability. Previous studies have reported various regeneration methods, such as using HCl (Awual *et al.* 2016), NaCl (Zhou *et al.* 2010) and NaOH (Liu *et al.*

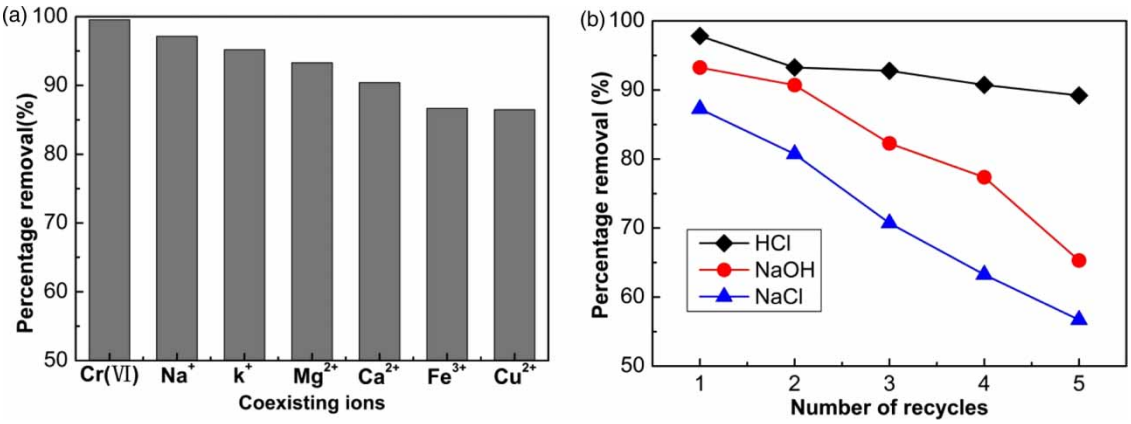

Figure 9 | (a) Effect of coexisting anions on Cr(VI) adsorption by CeO_2@ZSM-5; (b) number of reuses of CeO_2@ZSM-5 for Cr(VI) adsorption.

2017; Setshedi *et al.* 2013). In this study, the regeneration of CeO_2@ZSM-5 was tested using NaOH (0.1 M), NaCl (0.1 M) and HCl (0.1 M), all stirred for 1 hour at 25 °C. As shown in Figure 9(b), the initial efficiency was 99.56%, and then 89.2%, 65.2%, 52.7% after five regeneration cycles when using HCl, NaOH, NaCl as the eluent, respectively. The result showed that CeO_2@ZSM-5 could be easily regenerated and had a high recyclability over multiple cycles, with the best eluent being HCl (0.1 M).

Comparison studies

In order to justify the validity of CeO_2@ZSM-5 as a good adsorbent for the removal of Cr(VI), we carried out a comparison with previously published similar studies. As shown in Table 7, we compared various items such as initial concentration, contact time, adsorption capacity, percentage removal and number of reuses. In this study, for the purpose of reducing low concentration of Cr(VI) in aqueous solution, the initial concentration of metal ions was only 0.6 mg/L, which caused a lower adsorption capacity when compared with other works, which had an initial concentration greater than 50 mg/L. Even so, the percentage removal of CeO_2@ZSM-5 in our work was the highest. It can be seen that the percentage removal of Cr(VI) onto CeO_2@ZSM-5 was 89.2% after five regeneration cycles, a better regenerative effect than other adsorbents. What is more, it provided the shortest reaction time. Beyond those, other advantages such as easy preparation and lower cost made CeO_2@ZSM-5 a better prospect.

CONCLUSIONS

In this study, CeO_2 was loaded onto ZSM-5 by impregnation and used for the removal of Cr(VI) in low concentrations in aqueous solution (the concentration of Cr(VI) ranged from 0.2 to 1 mg/L). The structural order and textural properties of ZSM-5 and CeO_2@ZSM-5 were examined by XRD, BET, SEM-EDX, FTIR and XPS. The effects of important parameters such as pH, adsorbent dose, initial concentration and contact time of Cr(VI) were studied and the

Table 7 | Comparison of adsorption capacities of different adsorbents towards Cr(VI)

Adsorbent	Initial concentration (mg/L)	Contact time (min)	q_e (mg/g)	Percentage removal	Number of reuses	Percentage removal after reuse	Reference
Oxidized activated carbon	50	24 × 60	5.59	41.56%	–	–	Al-Othman *et al.* (2012)
Activated carbon	80	120	27.64	69.10%	–	–	Alothman *et al.* (2013)
ZrO_2/Fe_3O_4/chitosan	70	120	–	84.70%	6	–	Kumar *et al.* (2016)
CN-cl-PL(AA)NHG	60	180	19.80	72.30%	–	–	Sharma *et al.* (2017)
CeO_2@ZSM-5	0.6	70	0.24	99.56%	5	89.2%	This work

optimal conditions were set at 3, 5 g/L, 0.6 mg/L and 70 min, respectively, resulting in a removal rate of Cr(VI) was 99.56%. The Freundlich isotherm showed better agreement with the experimental data ($R^2 = 0.9941$) and the maximum adsorption capacity obtained from the Langmuir isotherm was 0.2392 mg/g. Kinetic studies indicate that adsorption equilibrium data fitted well with the pseudo-second-order model and the thermodynamic parameters showed the endothermic and spontaneous nature of the adsorption process. The competitive ions had only a small adverse effect of the adsorption of Cr(VI) onto CeO_2@ZSM-5. This adsorbent was easily recovered by desorption in 0.1 M HCl. Recycling experiments showed that the CeO_2@ZSM-5 still possessed high Cr(VI) adsorption efficiency and good stability after five cycles, which would enhance the economics of practical applications for the removal of Cr(VI) from wastewater.

ACKNOWLEDGEMENTS

This work was supported by the Natural Science Foundation of Hebei Province (E2016208116), the Science and Technology Plan of Hebei Province (15274208D) and the PhD startup fund.

REFERENCES

Al-Othman, Z. A., Ali, R. & Naushad, M. 2012 Hexavalent chromium removal from aqueous medium by activated carbon prepared from peanut shell: adsorption kinetics, equilibrium and thermodynamic studies. *Chemical Engineering Journal* **184** (2), 238–247. DOI: 10.1016/j.cej.2012.01.048.

Alothman, Z. A., Naushad, M. & Ali, R. 2013 Kinetic, equilibrium isotherm and thermodynamic studies of Cr(VI) adsorption onto low-cost adsorbent developed from peanut shell activated with phosphoric acid. *Environ. Sci. Pollut. Res. Int.* **20** (5), 3351–3365. DOI: 10.1007/s11356-012-1259-4.

Alqadami, A. A., Naushad, M., Alothman, Z. A. & Ghfar, A. A. 2017 Novel metal-organic framework (MOF) based composite material for the sequestration of U(VI) and Th(IV) metal ions from aqueous environment. *Acs. Appl. Mater. Interfaces.* 36026–36037. DOI: 10.1021/acsami.7b10768.

Awual, M. R., Hasan, M. M., Eldesoky, G. E., Khaleque, M. A., Rahman, M. M. & Naushad, M. 2016 Facile mercury detection and removal from aqueous media involving ligand impregnated conjugate nanomaterials. *Chemical Engineering Journal* **290**, 243–251. DOI: 10.1016/j.cej.2016.01.038.

Choi, H. J., Yu, S. W. & Kim, K. H. 2016 Efficient use of Mg-modified zeolite in the treatment of aqueous solution contaminated with heavy metal toxic ions. *Journal of the Taiwan Institute of Chemical Engineers* **63**, 482–489. DOI: 10.1016/j.jtice.2016.03.005.

Dai, M., Xia, L., Song, S., Peng, C. & Lopez-Valdivieso, A. 2016 Adsorption of As(V) inside the pores of porous hematite in water. *Journal of Hazardous Materials* **307**, 312–317. DOI: 10.1016/j.jhazmat.2016.01.008.

Djeribi, R. & Hamdaoui, O. 2008 Sorption of copper(II) from aqueous solutions by cedar sawdust and crushed brick. *Desalination* **225** (1), 95–112. DOI: 10.1016/j.desal.2007.04.091.

Gopalakrishnan, A., Krishnan, R., Thangavel, S., Venugopal, G. & Kim, S. J. 2015 Removal of heavy metal ions from pharma-effluents using graphene-oxide nanosorbents and study of their adsorption kinetics. *Journal of Industrial & Engineering Chemistry* **30**, 14–19. DOI: 10.1016/j.jiec.2015.06.005.

Hall, K. R., Eagleton, L. C., Acrivos, A. & Vermeulen, T. 1966 Pore- and solid-diffusion kinetics in fixed-bed adsorption under constant-pattern conditions. *Industrial & Engineering Chemistry Fundamentals* **5** (2), 587–594. DOI: 10.1021/i160018a011.

Kenawy, E. R., Ghfar, A. A., Naushad, M., Alothman, Z. A., Habila, M. A. & Albadarin, A. B. 2017 Efficient removal of Co(II) metal ion from aqueous solution using cost-effective oxidized activated carbon: kinetic and isotherm studies. *Desalination & Water Treatment* **70**, 220–226. DOI: 10.5004/dwt.2017.20534.

Kumar, A., Guo, C., Sharma, G., Pathania, D., Mu, N., Kalia, S. & Dhiman, P. 2016 Magnetically recoverable ZrO_2/Fe_3O_4/chitosan nanomaterials for enhanced sunlight driven photoreduction of carcinogenic Cr(VI) and dechlorination & mineralization of 4-chlorophenol from simulated waste water. *RSC Advances.* **6** (16), 13251–13263. DOI: 10.1039/C5RA23372.

Liu, J., Cao, J., Hu, Y., Han, Y. & Zhou, J. 2017 Adsorption of phosphate ions from aqueous solutions by a CeO_2 functionalized Fe_3O_4@SiO_2 core-shell magnetic nanomaterial. *Water Science & Technology* 2867–2875. DOI: 10.2166/wst.2017.412.

Mubarak, N. M., Sahu, J. N., Abdullah, E. C., Jayakumar, N. S. & Ganesan, P. 2016 Microwave-assisted synthesis of multi-walled carbon nanotubes for enhanced removal of Zn(II) from wastewater. *Research on Chemical Intermediates* 1–25. DOI: 10.1007/s11164-015-2209-9.

Naushad, M., Ahamad, T., Al-Maswari, B. M., Alqadami, A. A. & Alshehri, S. M. 2017 Nickel ferrite bearing nitrogen-doped mesoporous carbon as efficient adsorbent for the removal of highly toxic metal ion from aqueous medium. *Chemical Engineering Journal.* DOI: 10.1016/j.cej.2017.08.079.

Naushad, M., Ahamad, T., Sharma, G., Al-Muhtaseb, A. A. H., Albadarin, A. B., Alam, M. M., Alothman, Z. A., Alshehri, S. M. & Ghfar, A. A. 2016 Synthesis and characterization of a new starch/SnO_2 nanocomposite for efficient adsorption of toxic Hg^{2+} metal ion. *Chemical Engineering Journal* **300**, 306–316. DOI: 10.1016/j.cej.2016.04.084.

Rao, M., Parwate, A. V. & Bhole, A. G. 2002 Removal of Cr^{6+} and Ni^{2+} from aqueous solution using bagasse and fly ash. *Waste*

Management **22** (7), 821–830. DOI: 10.1016/S0956-053X(02)00011-9.

Rivas, B. D., Sampedro, C., Ramos-Fernández, E. V., López-Fonseca, R., Gascon, J., Makkee, M. & Gutiérrez-Ortiz, J. I. 2013 Influence of the synthesis route on the catalytic oxidation of 1,2-dichloroethane over CeO_2/H-ZSM5 catalysts. *Applied Catalysis A General* **456** (6), 96–104. DOI: 10.1016/j.apcata.2013.02.026.

Salerno, A., Pitault, I., Devers, T., Pelletier, J. & Briançon, S. 2017 Model-based optimization of parameters for degradation reaction of an organophosphorus pesticide, paraoxon, using ceo_2 nanoparticles in water media. *Environmental Toxicology & Pharmacology* **53** (6), 18. DOI: 10.1016/j.etap.2017.04.020.

Setshedi, K. Z., Bhaumik, M., Songwane, S., Onyango, M. S. & Maity, A. 2013 Exfoliated polypyrrole-organically modified montmorillonite clay nanocomposite as a potential adsorbent for Cr(VI) removal. *Chemical Engineering Journal* **222** (8), 186–197. DOI: 10.1016/j.cej.2013.02.061.

Sharma, G., Naushad, M., Almuhtaseb, A. H., Kumar, A., Khan, M. R., Kalia, S., Shweta, Bala, M. & Sharma, A. 2017 Fabrication and characterization of chitosan-crosslinked-poly (alginic acid) nanohydrogel for adsorptive removal of Cr(VI) metal ion from aqueous medium. *International Journal of Biological Macromolecules* **95**. DOI: 10.1016/j.ijbiomac.2016.11.072.

Wu, L., Fang, S., Ge, L., Han, C., Qiu, P. & Xin, Y. 2015 Facile synthesis of Ag@CeO_2 core-shell plasmonic photocatalysts with enhanced visible-light photocatalytic performance. *Journal of Hazardous Materials* **300**, 93–103. DOI: 10.1016/j.jhazmat.2015.06.062.

Zhou, J. B., Wu, P. X., Zhi, D., Zhu, N. W., Li, P., Wu, J. H. & Wang, X. D. 2010 Polymeric Fe/Zr pillared montmorillonite for the removal of Cr(VI) from aqueous solutions. *Chemical Engineering Journal* **162** (3), 1035–1044. DOI:10.1016/j.cej.2010.07.016.

First received 10 January 2018; accepted in revised form 23 March 2018. Available online 9 April 2018